

POINT PROCESS REGRESSION

Álvaro Gajardo and Hans-Georg Müller

Department of Statistics

University of California, Davis

Davis, CA 95616 U.S.A.

ABSTRACT

Point processes in time have a wide range of applications that include the claims arrival process in insurance or the analysis of queues in operations research. Due to advances in technology, such samples of point processes are increasingly encountered. A key object of interest is the local intensity function. It has a straightforward interpretation that allows to understand and explore point process data. We consider functional approaches for point processes, where one has a sample of repeated realizations of the point process. This situation is inherently connected with Cox processes, where the intensity functions of the replications are modeled as random functions. Here we study a situation where one records covariates for each replication of the process, such as the daily temperature for bike rentals. For modeling point processes as responses with vector covariates as predictors we propose a novel regression approach for the intensity function that is intrinsically nonparametric. While the intensity function of a point process that is only observed once on a fixed domain cannot be identified, we show how covariates and repeated observations of the process can be utilized to make consistent estimation possible, and we also derive asymptotic rates of convergence without invoking parametric assumptions.

Key words and phrases: Cox Process, Fréchet Regression, Intensity Function, Nonparametric Regression, Wasserstein Metric

Research supported by NIH ECHO and NSF DMS-1712864

1. Introduction

Temporal point processes are encountered in insurance in the form of the claim arrival process, risk processes and ruin theory which targets the solvency of the insurer (Mikosch 2009); queue theory in operations research (Daley and Vere-Jones 2003); seismology; demand patterns in bike sharing systems (Gervini and Khanal 2019); or bid arrivals in online auctions (Reddy and Dass 2006; Shmueli et al. 2007). Single realizations of point processes have been well studied in the literature (Cox and Isham 1980; Diggle et al. 2013). One important target is the intensity function, due to its straightforward interpretation as the rate of occurrence of points per unit time (Daley and Vere-Jones 2003). In the context of seismology, one expects the intensity function of the aftershock arrival process to depend on the size of the earthquake that triggered the aftershocks. This exemplifies point process data for which the intensity function depends on covariates, and provides the motivation to develop flexible nonparametric methods for such data. Specifically, we propose a nonparametric regression method for point processes as responses, coupled with Euclidean predictors in \mathbb{R}^p .

In the context of stationary Cox processes (Cox and Isham 1980), nonparametric kernel estimation of the intensity function for just one observed point process has been proposed (Diggle 1985), connecting this problem to kernel density estimation. However, when one has just one realization of the point process, no consistent estimator of the intensity function exists (Zhang and Kou 2010), due to the unavailability of a consistent estimator of the scale factor of the intensity function. In other work that explores the interface of spatio-temporal point processes and functional data analysis, Li and Guan (2014) proposed a semi-parametric generalized linear mixed model with a latent process component, and established asymptotic properties under increasing domain asymptotics, a design assumption that is commonly used for spatial processes. We consider here a different scenario, where replications of a temporal point process are available, along with an Euclidean covariate $X \in \mathbb{R}^p$. A previous replicated point process regression approach (Lawless 1987) also dealt with repeatedly observed non-homogeneous Poisson processes as responses; however this previous approach relied heavily on parametric specifications, for which diagnostics is very difficult, whereas we aim here at a flexible nonparametric approach that applies much more generally.

In the context of Cox processes, where the intensity function $\Lambda(x)$ is a positive locally integrable random function, a common approach when dealing with repeatedly observed point processes (but without a covariate X) has been to combine likelihood methods and techniques from Functional Data Analysis (Bouzas et al. 2006; Bouzas and Ruiz-Fuentes 2015; Gervini 2017; Gervini and Khanal 2019). For example, in Gervini (2017) a Karhunen-Loève expansion (Grenander 1950; Kleffe 1973) was applied to the log intensity random functions,

$$\log(\Lambda(t)) = \mu(t) + \sum_{k=1}^{\infty} U_k \phi_k(t), \quad 0 \leq t \leq T,$$

where $0 < T < \infty$ and $\mu \in L^2([0, T])$ is the mean function, the U_k are uncorrelated random variables and ϕ_1, ϕ_2, \dots form an orthonormal basis of $L^2([0, T])$. Then, by using techniques such as Functional Principal Component Analysis (FPCA), a truncated version of the expansion is considered with only p components and thus functional problem of estimating μ and the ϕ_k is reduced to a multivariate approach, modeling the functions in a finite dimensional function space of basis functions like B-splines. Distributional assumptions such as Gaussianity on the U_k are also introduced in order to justify a likelihood approach to obtain estimates for the basis coefficients.

Similarly, [Wu et al. \(2013\)](#) proposed a functional approach that decomposes the intensity function into an intensity factor and a shape function and then performed a Karhunen-Loève expansion for the shape function, borrowing strength across the replications. These methods face constraints due to the non-negative nature of the intensity function and cannot be directly extended to establish regression models for point processes. Since the random intensity functions are not observed, the event arrival times are used in the estimation procedures. For Cox processes, the key relation that allows this is that conditional on n events occurring in an interval $[0, T]$ and $\Lambda = \lambda$, the unordered arrival times form an i.i.d. sample with density $\lambda / \int \lambda$ which is a well known property for non-homogeneous Poisson processes ([Daley and Vere-Jones 2003](#)). Furthermore, as noted in [Wu et al. \(2013\)](#), the intensity function λ can be decomposed into a shape function $f = \lambda / \int \lambda$ and an intensity factor $\tau = \int \lambda$. This decomposition is the key relationship that will enable us to split the problem of estimating the intensity function conditional on covariates into two parts: Estimating the conditional shape function and estimating the conditional intensity factor of the process.

The proposed regression approach for the intensity function of replicated temporal point processes on Euclidean predictors utilizes conditional Fréchet means ([Petersen and Müller 2019](#)) for a suitable metric on the space of intensity functions, where this metric can be decomposed into two parts, one that quantifies differences in shape and a second part that quantifies differences in the intensity factors. As we need to estimate the density function associated with the arrival times of the point process, our asymptotic consistency results for the intensity function also utilize tools that were developed in [Panaretos and Zemel \(2016\)](#). The common assumption of letting the observation window $T \rightarrow \infty$ is often not applicable, which includes the data we consider below to motivate our methods. Therefore, we consider an asymptotic framework where T remains fixed and the number of replicates of the point process increases.

While in general the intensity function of a doubly stochastic Poisson process cannot be consistently estimated as it is random, we demonstrate here that the situation is different for point processes conditional on a covariate, as we establish asymptotic consistency with rates of convergence for conditional intensity functions. We illustrate the implementation of the proposed point process regression with simulations and show that it leads to well interpretable results for the Chicago Divvy bike trips

and the New York yellow taxi trips data. An extended application to the earthquake aftershock process in Chile is presented in Supplement S.6.

The main innovations provided in this paper are: (1) We develop the first fully nonparametric regression method that features point processes as responses with Euclidean predictors; (2) We obtain asymptotic rates of convergence for conditional intensity functions, while such a result is not achievable for intensity functions unconditionally; (3) Our approach does not require functional principal components and does not require distributional assumptions, as it is not utilizing likelihood; (4) The proposed approach is shown to work well in relevant applications. The framework of Fréchet regression for intensity space is introduced in section 2, estimation and theory with convergence results are presented in sections 3 and 4. Simulation results can be found in section 5 and data illustrations and extensions in section 6. All proofs are in the Supplement.

2. The space of intensity functions

Let $\{N(t), t \geq 0\}$ be a temporal point process where $N(t)$ represents the number of events that occur in the time interval $[0, t]$ and $N(0) = 0$. We suppose that $N(t)$ is observed on the time window $[0, T]$ for some endpoint $T > 0$, and is such that $m(t) := E(N(t)) < \infty$ for $0 \leq t \leq T$. In the context of replicated point processes that we consider here, it is natural to work within the framework of a doubly stochastic Poisson process (N, Λ) where one assumes that there is an underlying stochastic intensity process $\Lambda(t)$ that generates non-negative integrable functions on $[0, T]$ such that conditional on a realization $\Lambda = \lambda$, $N|\Lambda = \lambda$ is a non-homogeneous Poisson process with intensity function λ (Cox and Isham 1980). A feature that greatly facilitates analysis of such processes (Wu et al. 2013; Gervini 2017; Gervini and Khanal 2019; Panaretos and Zemel 2016) is the fact that a Poisson process has the order statistics property, i.e., conditional on m events being observed in $[0, T]$, the successive event times are distributed as the order statistics of m independent and identically distributed random variables with a density that is proportional to the intensity function (Daley and Vere-Jones 2003).

Denoting the space of intensity functions as

$$\Omega = \left\{ \Lambda: [0, T] \rightarrow \mathbb{R}^+ \text{ such that } \int_0^T \Lambda(t) dt < \infty \right\},$$

two key quantities for each $\Lambda \in \Omega$ are the *intensity factor*, a scalar

$$\tau := \int_0^T \Lambda(t) dt,$$

which is the expected number of events in $[0, T]$, conditional on $\Lambda(\cdot)$; and the *shape function*

$$f(t) := \frac{\Lambda(t)}{\tau}, \quad \text{where} \quad \int_0^T f(t) dt = 1, \quad f(t) \geq 0, \quad t \in [0, T],$$

which is a density function. Hence, $\Lambda(\cdot) = \tau f(\cdot)$ and since there is a one-to-one correspondence between Λ and (τ, f) we may regard Ω as a product space $\Omega = \Omega_{\mathcal{T}} \times \Omega_{\mathcal{F}}$ where $\Omega_{\mathcal{T}} = (0, \infty)$ and

$$\Omega_{\mathcal{F}} = \{f: [0, T] \rightarrow \mathbb{R} \text{ such that } f > 0 \text{ and } \int_0^T f(t)dt = 1\}.$$

Furthermore, if we endow $\Omega_{\mathcal{T}}$ and $\Omega_{\mathcal{F}}$ metrics $d_{\mathcal{T}}$ and $d_{\mathcal{F}}$, respectively, we may regard (Ω, d) as a product metric space $(\Omega_{\mathcal{T}}, d_{\mathcal{T}}) \times (\Omega_{\mathcal{F}}, d_{\mathcal{F}})$, where

$$d((\tau_1, f_1), (\tau_2, f_2)) := \sqrt{d_{\mathcal{T}}^2(\tau_1, \tau_2) + d_{\mathcal{F}}^2(f_1, f_2)}. \quad (1)$$

In the context of metric geometry such product metric spaces for which the distance arises as an l^2 -type norm between the underlying metrics have been extensively studied. In particular, it is well known that Ω is a geodesic space if and only if $\Omega_{\mathcal{T}}$ and $\Omega_{\mathcal{F}}$ are geodesic spaces (Burago et al. 2001). This decomposition enables us to measure differences in shape and magnitude separately. We choose the Euclidean metric $d_{\mathcal{T}}(\tau_1, \tau_2) := d_E(\tau_1, \tau_2)$ and the Wasserstein metric $d_{\mathcal{F}}(f_1, f_2) := d_W(\mu_1, \mu_2)$, where the latter has been shown to be a most useful metric in practical applications (Bolstad et al. 2003) and for two probability measures μ_1, μ_2 on $[0, T]$ with associated density functions f_1, f_2 and quantile functions Q_1, Q_2 is defined as (Villani 2003)

$$d_W^2(\mu_1, \mu_2) = d_{L^2}^2(Q_1, Q_2) = \int_0^1 (Q_1(t) - Q_2(t))^2 dt.$$

where we assume throughout that these quantities exist and are well defined. A basic notion for statistical modeling is the mean of a random variable, where for random objects in a metric space $(\tilde{\Omega}, \tilde{d}, P)$ it has proved advantageous to adopt the barycenter or Fréchet mean (Fréchet 1948), defined as $w_{\oplus} := \arg \min_{w \in \tilde{\Omega}} E(\tilde{d}^2(Y, w))$ where $Y \in \tilde{\Omega}$ is a random object. The Fréchet mean may be regarded as an extension of the standard concept of mean in Euclidean space to abstract metric spaces in the sense that when $\tilde{\Omega}$ is a convex subset of the Euclidean space and \tilde{d} is the Euclidean metric, then the ordinary mean and the Fréchet mean coincide. The barycenter and its estimation has attracted much interest for distribution spaces with the Wasserstein metric (Aguech and Carlier 2011; Cazelles et al. 2018; Bigot et al. 2018; Panaretos and Zemel 2016; Panaretos and Zemel 2019); we adopt these spaces here for the shape part of the intensity function.

3. Framework for Intensity Function Regression

3.1 Preliminaries

Our goal is to model the regression relation between random intensity functions Y in the above space (Ω, d) as responses and an Euclidean predictor $X \in \mathbb{R}$, for which we adopt the recently developed framework of Fréchet regression (Petersen and Müller 2019), which can be viewed as a generalization

of Fréchet means to the more general notion of conditional Fréchet means. Formally, define the regression or conditional intensity function $m_{\oplus}(x)$ as

$$m_{\oplus}(x) := \arg \min_{w \in \Omega} M_{\oplus}(w, x), \quad M_{\oplus}(w, x) := E(d^2(Y, w)|X = x),$$

where $w = (\tau_0, f_0) \in \Omega = \Omega_{\mathcal{T}} \times \Omega_{\mathcal{F}}$ and $Y = (\tau, f) \in \Omega_{\mathcal{T}} \times \Omega_{\mathcal{F}}$, so that by (1),

$$M_{\oplus}(w, x) = E(d_{\mathcal{T}}^2(\tau, \tau_0)|X = x) + E(d_{\mathcal{F}}^2(f, f_0)|X = x).$$

Hence, the optimization problem is separable with optimal solution $m_{\oplus}(x) = (\tau_{\oplus}(x), f_{\oplus}(x))$, where

$$\tau_{\oplus}(x) = \arg \inf_{\tau_0 \in \Omega_{\mathcal{T}}} E(d_{\mathcal{T}}^2(\tau, \tau_0)|X = x) = \max\{E(\tau|X = x), 0\}; \quad (2)$$

$$f_{\oplus}(x) = \arg \inf_{f_0 \in \Omega_{\mathcal{F}}} E(d_{\mathcal{F}}^2(f, f_0)|X = x). \quad (3)$$

Note that since we measure the differences in the intensity factor from the changes in shape separately, the order of magnitude between the two metrics is not relevant. More precisely, $m_{\oplus}(x)$ remains the same for weighted metrics $d_{\lambda}^2 = \alpha d_{\mathcal{T}}^2 + \beta d_{\mathcal{F}}^2$ with $\alpha, \beta > 0$.

A basic difficulty is that the function $\Lambda(\cdot)$ is not observed. If sufficiently many arrival times are observed for each replication of the point process, then it is well known that consistent estimation of the density function f may be achieved by classical density estimation techniques (Diggle 1985; Panaretos and Zemel 2016), while some work-arounds exist for sparsely observed point processes (Wu et al. 2013). However, the situation is much less benign regarding estimation of the intensity parameter τ . It would be natural to employ the total count $N(T)$, which is conditionally unbiased for τ in the sense that $E(N(T)|\Lambda) = \tau$ but is not (conditionally) consistent as $\text{Var}(N(T)|\Lambda) = \tau$. When just one replicate of a point process is observed, consistent estimation of the intensity function is therefore not possible. Further motivating conditional intensity function modeling, we show in the following that the situation is different when considering conditional intensity functions. We demonstrate that the counts $N_i(T)$ can be used as initial estimates for the random intensity factors τ_i , from which consistent estimators can then be derived. This phenomenon is analogous to classical linear regression modeling, where one has errors in the responses and yet consistent estimation of the conditional expectation that corresponds to the true regression function is achieved, and it provides strong motivation for the proposed methods and the consideration of conditional point processes.

3.2 Local Regression for Intensity Functions

Suppose that a sample of replicates (X_i, N_i, f_i, τ_i) is drawn from the joint distribution of (X, N, f, τ) , $i = 1, \dots, n$, where $N|\Lambda = f \times \tau$ is a Poisson process with intensity function $\lambda = f \times \tau$. We employ empirical weights from local linear regression (Fan and Gijbels 1996) that are inherent to the local

Fréchet regression approach (Petersen and Müller 2019), and are given by

$$s_{in}(x, h) = \frac{1}{\hat{\sigma}_0^2} K_h(X_i - x) [\hat{u}_2 - \hat{u}_1(X_i - x)], \quad (4)$$

where $\hat{u}_j = n^{-1} \sum_{i=1}^n K_h(X_i - x)(X_i - x)^j$ with $j \in \{0, 1, 2\}$, $\hat{\sigma}_0^2 = \hat{u}_0 \hat{u}_2 - \hat{u}_1^2$ and $K_h(\cdot) = h^{-1} K(\cdot/h)$, the kernel K is a continuous and symmetric density function with support $[-1, 1]$, and $h = h_n$ is a sequence of bandwidths.

As we can factorize the response into a density function and an intensity factor, one regression component is the conditional mean $E(\tau|X = x)$. For estimating this quantity we employ local linear regression. If the τ_i were observed, then a naive estimator for (2) would be given by

$$\hat{\tau}_\oplus(x) = \max\{0, n^{-1} \sum_{i=1}^n s_{in}(x, h) \tau_i\}, \quad (5)$$

as local linear regression is a linear estimator, assigning weights $s_{in}(x, h)$ to the responses. However, this estimator is based on the intensity factors τ_i , which are not observed; we only observe the counts of arrivals $N_i(T)$ for each replicate of the point process. This difficulty can be resolved by noting that the observed counts $N_i(T)$ satisfy the relationship $E(N_i(T)|\Lambda_i) = \tau_i$, which enables us to replace τ_i by $N_i(T)$ in (5) since $E(N(T)|X) = E(E(N(T)|X, \Lambda)|X) = E(\tau|X)$ is on target. Hence, under suitable regularity conditions one readily obtains well known non-parametric convergence rates for the corresponding locally weighted least squares estimator of $\tau_\oplus(x)$ (2) (Fan and Gijbels 1996).

If the densities f_i associated with point processes N_i were completely observed, we could implement local Fréchet regression on the space of densities for (3) (Petersen and Müller 2019),

$$\hat{f}_\oplus(x) = \arg \min_{f_0 \in \Omega_{\mathcal{F}}} n^{-1} \sum_{i=1}^n s_{in}(x, h) d_{\mathcal{F}}^2(f_i, f_0). \quad (6)$$

We however only observe the arrival times, from which the densities f_i must be estimated, and this will induce an additional error that needs to be accounted for when analyzing the final estimator.

As noted by Cucala (2008), one of the main differences compared to classical density estimation techniques is that in the context of point processes we cannot let the number of observations go to infinity as it is a random feature of the point process itself. Instead it is useful to consider an asymptotic framework where the intensity factors τ_i diverge to infinity, while the observation window $[0, T]$ remains fixed; see also Panaretos and Zemel (2016) or Diggle and Marron (1988). This framework will be introduced in section 4. From now on, τ will denote a generic intensity factor such that $\tau_i = \int_0^T \Lambda_i(s) ds \stackrel{iid}{\sim} \tau$, $i = 1, \dots, n$.

The minimization problem (6) is easily solved by considering quantile functions. If Q_i is the quantile function corresponding to f_i , $i = 1, \dots, n$ and $\hat{Q}_\oplus(\cdot, x) : [0, 1] \rightarrow [0, T]$ is the quantile function corresponding to the density $\hat{f}_\oplus(x)$ in (6),

$$\hat{Q}_\oplus(\cdot, x) = \arg \min_{q \in Q(\Omega_{\mathcal{F}})} n^{-1} \sum_{i=1}^n s_{in}(x, h) \|Q_i - q\|_{L^2([0, 1])}^2,$$

where $Q(\Omega_{\mathcal{F}})$ is the space of quantile functions corresponding to densities in $\Omega_{\mathcal{F}}$. Standard properties of the $L^2([0, 1])$ inner product imply (Proposition 1 in [Petersen and Müller \(2019\)](#))

$$\hat{Q}_{\oplus}(\cdot, x) = \arg \min_{q \in Q(\Omega_{\mathcal{F}})} \|q - n^{-1} \sum_{i=1}^n s_{in}(x, h) Q_i\|_{L^2([0,1])}^2. \quad (7)$$

To discuss estimation of the Q_i , which are needed in (7) but are not directly available, it is helpful to consider auxiliary probability measures $\hat{\mu}_i$ on $[0, T]$ that correspond to the empirical measure of the arrival times when the total count $N_i(T) \geq 1$ and to the uniform measure on $[0, T]$ otherwise (see [Panaretos and Zemel 2016](#)). That is,

$$\hat{\mu}_i = \begin{cases} \frac{1}{N_i(T)} \sum_{j=1}^{N_i(T)} \delta_{Z_{ij}}, & \text{if } N_i(T) \geq 1 \\ \frac{1}{T} \mathcal{L}, & \text{if } N_i(T) = 0, \end{cases}$$

where Z_{ij} are the arrival times of the point process N_i and \mathcal{L} is the Lebesgue measure on $[0, T]$. For a probability measure μ on $[0, T]$ with cdf F_μ we consider its quantile function $Q_\mu(t) := \inf\{x \in [0, T] : F_\mu(x) \geq t\}$. Let $\hat{Q}_i := Q_{\hat{\mu}_i}$, then replacing Q_i by \hat{Q}_i in (7) leads to the empirical estimate

$$\tilde{Q}_{\oplus}(\cdot, x) := \arg \min_{q \in Q(\Omega_{\mathcal{F}})} \|q - n^{-1} \sum_{i=1}^n s_{in}(x, h) \hat{Q}_i\|_{L^2([0,1])}^2. \quad (8)$$

4. Asymptotic Results

4.1 Convergence of the Shape Function Estimates

Let $\tilde{f}_{\oplus}(x)$ be the density function corresponding to the quantile function $\tilde{Q}_{\oplus}(\cdot, x)$. Thus, $\tilde{f}_{\oplus}(x)$ corresponds to the empirical estimate for (6). We require the following assumptions, which guarantee that $Q(\Omega_{\mathcal{F}})$ is a closed and convex subset of the Hilbert space $L^2([0, 1])$, yielding existence and uniqueness of the naive and empirical estimators in (7) and (8), respectively.

(S1) Suppose that there exists $0 < M < L < \infty$ such that for all $Q \in Q(\Omega_{\mathcal{F}})$ and $x, y \in [0, 1]$

$$M|x - y| \leq |Q(x) - Q(y)| \leq L|x - y|$$

(S2) Suppose that for any $Q \in Q(\Omega_{\mathcal{F}})$ it holds that $Q(0) = 0$ and $Q(1) = T$.

These assumptions are needed to ensure that the quantile functions do not increase too rapidly or too slowly, which is equivalent to constraining the density functions to be well behaved and bounded away from zero.

Lemma 1. *Under (S1) – (S2), $Q(\Omega_{\mathcal{F}})$ is a closed and convex set on the Hilbert space $L^2([0, 1])$.*

Regarding the convergence of $\tilde{f}_\oplus(x)$ towards $f_\oplus(x)$ in the Wasserstein metric, by the triangle inequality

$$d_{\mathcal{F}}(f_\oplus(x), \tilde{f}_\oplus(x)) \leq d_{\mathcal{F}}(f_\oplus(x), \hat{f}_\oplus(x)) + d_{\mathcal{F}}(\hat{f}_\oplus(x), \tilde{f}_\oplus(x)), \quad (9)$$

and for the term $d_{\mathcal{F}}(\hat{f}_\oplus(x), \tilde{f}_\oplus(x))$ we observe that properties of the orthogonal projection on a closed and convex set in the Hilbert space $L^2([0, 1])$ imply that

$$d_{\mathcal{F}}(\tilde{f}_\oplus(x), \hat{f}_\oplus(x)) = \|\tilde{Q}_\oplus(\cdot, x) - \hat{Q}_\oplus(\cdot, x)\|_{L^2([0, 1])} \leq n^{-1} \sum_{i=1}^n |s_{in}(x, h)| \|\hat{Q}_i - Q_i\|_{L^2([0, 1])}. \quad (10)$$

Therefore, convergence hinges on consistent estimation of the quantile functions Q_i . We consider the following asymptotic framework:

1. A first random mechanism generates pairs of predictors X_i and intensity functions Λ_i , $(X_1, \Lambda_1), \dots, (X_n, \Lambda_n) \stackrel{iid}{\sim} (X, \Lambda)$ which encapsulates the dependency between these random quantities. While the X_i are observed, the Λ_i are not observed.
2. Given the random intensity functions Λ_i , a second independent random mechanism then generates the observable number of arrivals $N_i^{(n)}(T)$ and the arrival times $Z_{i1}, \dots, Z_{iN_i^{(n)}(T)}$ for the i -th point process $N_i^{(n)}$, $i = 1, \dots, n$.
3. Conditional on $N_i^{(n)}(T)$, the (unordered) arrival times $Z_{i1}, \dots, Z_{iN_i^{(n)}(T)} \stackrel{iid}{\sim} f_i$.
4. Given the random intensity function Λ_i , $N_i^{(n)}(T) \sim \mathcal{P}(\alpha_n \tau_i)$ for a positive sequence $\alpha_n \rightarrow \infty$.

We note that conditions 1-3 are standard in the context of Cox processes while condition 4 allows for the observable number of arrivals $N_i^{(n)}(T)$ to diverge as n increases and to avoid empty point processes (Panaretos and Zemel 2016), which is the key for consistent estimation of Q_i by using the empirical measure of the arrival times. For simplicity of notation, the dependency of the process $N_i^{(n)}$ on n is dropped. The following result shows that the second term on the right hand side of (9) is $O_p(\alpha_n^{-1/4})$ provided that the support of τ is bounded away from zero and α_n grows fast enough.

Proposition 1. *Suppose that (S1) and (S2) hold, $\tau \geq 1$ and $\frac{\alpha_n}{\log n} \rightarrow \infty$ as $n \rightarrow \infty$. Then*

$$d_{\mathcal{F}}(\hat{f}_\oplus(x), \tilde{f}_\oplus(x)) = O_p(\alpha_n^{-1/4}).$$

The term $d_{\mathcal{F}}(f_\oplus(x), \hat{f}_\oplus(x))$ on the right hand side of (9) was shown to be $O_p(n^{-2/5})$ under the following regularity condition (Petersen and Müller 2019):

(L1) The marginal density f_X of X , as well as the conditional densities g_y of $X|\tilde{Y} = y$, exist for $\tilde{Y} \in \Omega_{\mathcal{F}}$ and are twice continuously differentiable, the latter for all $y \in \Omega_{\mathcal{F}}$, and $\sup_{x,y} |g_y''(x)| < \infty$. Additionally, for any open $U \subset \Omega_{\mathcal{F}}$, $\int_U dF_{\tilde{Y}|X}(x, y)$ is continuous as a function of x .

Summarizing these results, we obtain

Theorem 1. Suppose that (S1), (S2) and (L1) hold, $\tau \geq 1$, the density function satisfies $f_X(\cdot) > 0$, $\frac{\alpha_n}{\log n} \rightarrow \infty$ as $n \rightarrow \infty$ and $h = h_n \sim c_0 n^{-1/5}$ for some constant $c_0 > 0$. Then

$$d_{\mathcal{F}}(f_{\oplus}(x), \tilde{f}_{\oplus}(x)) = O_p(n^{-2/5} + \alpha_n^{-1/4}).$$

Accordingly, consistent estimation in the Wasserstein metric for the shape part of the conditional intensity function can be achieved at the rate $O_p(n^{-2/5})$ as long as $n^{8/5}\alpha_n^{-1}$ is bounded above. If this assumption holds, the well known rate of convergence for local linear regression with real valued responses is thus obtainable. However, the consistent estimation of conditional intensity factors places an upper bound on the sequence α_n that is slower than $n^{8/5}$. Thus, if one aims at both conditional shape function and conditional intensity factor estimation, the rate is slower; see Corollary 1.

4.2 Convergence of the Intensity Factor Estimates

In the increasing asymptotics framework that was introduced in the previous section, we assumed that there is a common intensity factor multiplier α_n such that $\alpha_n \rightarrow \infty$ as $n \rightarrow \infty$. This led to consistent estimation of the conditional intensity functions for the shape function part of the intensity function, where one works in the density space $\Omega_{\mathcal{F}}$. Since intensity functions can be factorized into a shape part, which corresponds to a density function, and an intensity factor, it remains to construct an estimator for the intensity factor (2) conditional on predictors X .

It turns out that this is a challenge, as an estimator for (5) is not easily available. This is because in order to estimate the shape functions consistently, it is necessary to assume that the expected number of events increases without bound. We show in the following how this challenge can be overcome and consistent estimation of $E(\tau|X)$ is nevertheless still possible up to the constant $E(\tau)$, so that relative intensities can be estimated consistently. The key to achieve this is to utilize the average observed number of arrivals $\bar{N}(T) := n^{-1} \sum_{i=1}^n N_i(T)$. We require the following regularity conditions.

- (LL1) The regression function $m(x) = E(\tau|X = x)$, the density function $f_X(x) > 0$ of X and $\sigma^2(x) = E(e^2|X = x)$, where $e = \tau - m(X)$, are twice continuously differentiable in x .
- (LL2) For the bandwidth sequence h , $nh^5 = O(1)$, as $n \rightarrow \infty$.
- (LL3) There exists $\delta > 0$ and $\bar{\sigma} > 0$ such that $E(|e|^{2+\delta}|X) \leq \bar{\sigma}$, for all predictors X .

We note that assumption (LL1) is a basic smoothness assumption that is needed to expand the bias for local linear smoothing, while (LL2) is also a common assumption and implies that as $n \rightarrow \infty$ and for $q \in \mathbb{N}$, we have $nh^q \rightarrow \infty$ if $0 \leq q \leq 4$ and $nh^q \rightarrow 0$ for $q > 5$. Assumption (LL3) will be used for an application of the central limit theorem.

Our main result on conditional intensity estimation is as follows.

Theorem 2. Under (LL1) – (LL3), suppose that $1 \leq \tau \leq M_1$ for a constant $M_1 < \infty$, $\alpha_n = O(n^{4/5})$ and $\frac{\alpha_n}{\log n} \rightarrow \infty$ as $n \rightarrow \infty$. Then

$$\max \left(0, \frac{n^{-1} \sum_{i=1}^n s_{in}(x, h) N_i(T)}{\bar{N}(T)} \right) = \frac{1}{E(\tau)} \tau_{\oplus}(x) + O_p(\alpha_n^{-1/2}).$$

This means that $\tau_{\oplus}(x)$ can still be consistently estimated up to the constant $E(\tau)$ by using the observable numbers of arrivals $N_i(T)$ of each replication of the point process instead of the true intensity factors τ_i , which are not observed. Furthermore, as the observed counts $N_i(T)$ grow with α_n as $n \rightarrow \infty$, we can stabilize the local linear estimator by employing comparisons against the average number of arrivals $\bar{N}(T)$. The assumptions require that α_n does not increase faster than $n^{4/5}$. This is due to the fact that local linear regression estimators with real valued responses are employed. These have a well known optimal rate of convergence $O_p(n^{-2/5})$ under mild assumptions, which is obtained under our assumptions if $\frac{\sqrt{\alpha_n}}{n^{2/5}} \rightarrow C$ for some $C > 0$ as $n \rightarrow \infty$.

4.3 Convergence of the Conditional Intensity Function Estimates

We are now in position to construct an estimate for the conditional intensity function by combining our previous results. Recall that the regression or conditional intensity function satisfies $m_{\oplus}(x) = \tau_{\oplus}(x) f_{\oplus}(x)$ where $\tau_{\oplus}(x)$ and $f_{\oplus}(x)$ are defined in (2) and (3), respectively, and

$$\tilde{\tau}_{\oplus}(x) = \max \left(0, \frac{n^{-1} \sum_{i=1}^n s_{in}(x, h) N_i(T)}{\bar{N}(T)} \right),$$

which corresponds to the estimate of $\tau_{\oplus}(x)$, up to the constant $E(\tau)$, as per Theorem 2.

Since $\Lambda_{\oplus}(x) = \tau_{\oplus}(x) f_{\oplus}(x)$, we obtain an estimate of $\Lambda_{\oplus}(x)$ by plugging in the previously obtained estimates of the intensity factor $\tau_{\oplus}(x)$ and of the shape function $f_{\oplus}(x)$, leading to

$$\hat{\Lambda}_{\oplus}(x) = \tilde{\tau}_{\oplus}(x) \tilde{f}_{\oplus}(x). \quad (11)$$

Here $\tilde{f}_{\oplus}(x)$ is the density corresponding to the quantile function defined in (8). This estimator is consistent for the conditional intensity function up to $E(\tau)$, as per the following result.

Corollary 1. Under the regularity conditions of Theorems 1 and 2, the estimate $\hat{\Lambda}_{\oplus}(x)$ of the conditional intensity function $m_{\oplus}(x)$ is consistent up to the constant $E(\tau)$ in the sense that

$$d(m_{\oplus}(x), E(\tau) \hat{\Lambda}_{\oplus}(x)) = O_p(\alpha_n^{-1/4}),$$

where $\frac{\alpha_n}{\log n} \rightarrow \infty$ and $\alpha_n = O(n^{4/5})$ as $n \rightarrow \infty$.

This result follows directly from Theorems 1 and 2. If the sequence α_n has a polynomial growth rate $\alpha_n/n^{\rho} \rightarrow C$ as $n \rightarrow \infty$ for some $\rho > 0$ and $C > 0$, then the assumptions on α_n require that

$\rho \in (0, 4/5]$ and the convergence rate in the Corollary is $O_p(n^{-\rho/4})$. The fastest convergence rate achievable is obtained when $\rho = 4/5$ which leads to $d(m_{\oplus}(x), E(\tau)\hat{\Lambda}_{\oplus}(x)) = O_p(n^{-1/5})$. In this case, the estimation of the intensity factor part, up to the constant $E(\tau)$, has the convergence rate $O_p(n^{-2/5})$ while for the shape part of the conditional intensity function the rate is slower and corresponds to $O_p(n^{-1/5})$.

5. Simulations

To assess the finite sample performance of the proposed conditional intensity function estimates, we constructed a generative model that produces simulated random intensity functions $\Lambda(\cdot) = f(\cdot)\tau$ along with an Euclidean predictor $X \in \mathbb{R}$. Let $Q(\cdot)$ be the quantile function corresponding to $f(\cdot)$. We consider the following regression model for f and τ on X : First a random rate parameter g is generated from a linear regression model $g = a_0 + b_0X + \epsilon$, where ϵ is independent of X and has a truncated normal distribution with mean zero, variance σ_0^2 and support $[c_0, d_0]$. Then $Q(\cdot)$ is generated as the quantile function of a truncated exponential random variable over $[0, T]$ with random rate g that depends on X . The choice of the constants a_0, b_0, c_0, d_0 is such that $a_0 + b_0x + \epsilon > 0$ for all x in the support of F_X . Conditional density functions f were constructed by transforming the respective conditional quantile functions Q at X . For the intensity factor τ , we consider a linear regression setting

$$E(\tau|X = x) = a_1 + b_1x,$$

such that the values on the right hand side are all positive.

The conditional intensity factors τ for covariate level X were obtained through a linear regression model $\tau = a_1 + b_1X + \varepsilon$, where ε is independent of X and has a truncated normal distribution with mean zero, variance σ_1^2 and support $[c_1, d_1]$. The choice of the constants above are such that $a_1 + b_1x + \varepsilon > 0$ for all x in the support of F_X .

Next, random samples of data (X_i, τ_i, Q_i) , $i = 1, \dots, n$, were generated following the above procedure where $X_i \sim \mathcal{U}(0, 1)$ and $a_0 = 0.7$, $b_0 = 0.9$, $\sigma_0 = 0.1$, $a_1 = 1.2$, $b_1 = 0.4$, $\sigma_1 = 0.1$, $c_0 = c_1 = -0.2$, $d_0 = d_1 = 0.2$ and $T = 1$. A triangular array of point processes was then obtained as follows: Conditional on (X_i, τ_i, Q_i) , the observable number of arrivals for the i -th point process $N_i(T)$ was sampled from a Poisson distribution with rate $\alpha_n \tau_i$, where $\alpha_n = 30n^{4/5}$. Then, conditional on $N_i(T)$ and Q_i , the arrival times were generated as an i.i.d. sample of size $N_i(T)$ with a truncated exponential density over $[0, T]$ of rate g_i , which has the quantile function Q_i . We generated Q_i over a dense grid on $[0, 1]$ and used the bandwidth sequence $h = h_n = n^{-1/5}$ for the local Fréchet regression step.

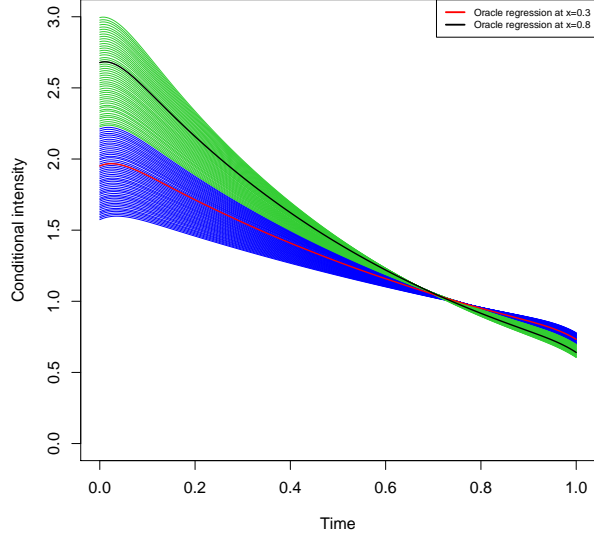


Figure 1: Conditional intensity functions in the simulation setting, displayed in blue for predictors $x \in [0, 0.5]$ and in green when $x \in [0.5, 1]$.

We ran 1000 simulations for sample sizes $n = 100, 200$ and 500 . For the r^{th} simulation, we measure the performance of the method by comparing against the ‘‘oracle’’ conditional intensity function with intensity factors $E(\tau|X = x)$ and shape (density) function defined through the corresponding quantile function $E(Q(\cdot)|X = x)$. The latter was approximated through a Monte Carlo approach where we average over 10,000 random quantiles Q_i generated at the predictor level x . Figure 1 shows the ‘‘oracle’’ regression function over a dense grid of predictor values.

Denoting by $\tilde{f}_\oplus^r(x)$ and $\tilde{\tau}_\oplus^r(x)$ the empirical estimates for the shape function and intensity factor parts of the conditional intensity function in the r -th simulation, respectively, we measured the quality of the estimation by integrated squared errors similar to Petersen and Müller (2019), using the metric as in (1). For computational details, we refer to Supplement S.5. Since $\tau_\oplus(x)$ can be consistently estimated up to the constant $E(\tau)$, we expect the estimates and $\tau_\oplus(x)$ to differ by a positive constant and the estimates $\tilde{\tau}_\oplus^r(x)$ of $\tau_\oplus(x)$ as in Theorem 2 by $E(\tau)$. This leads to

$$ISE_r = \int_5^6 \left\{ d_{L^2}^2(\tilde{Q}_\oplus(x), E(Q(\cdot)|X = x)) + d_E^2(E(\tau)\tilde{\tau}_\oplus^r(x), E(\tau|X = x)) \right\} dx = ISE_r^{\mathcal{F}} + ISE_r^{\mathcal{T}}.$$

The boxplots of $ISE_r^{\mathcal{F}}$ and $ISE_r^{\mathcal{T}}$ are presented in Figure 2. As sample size increases, these error estimates are seen to decrease towards 0. This indicates that the estimated conditional intensity functions converge to their true counterparts, up to the constant $E(\tau)$.

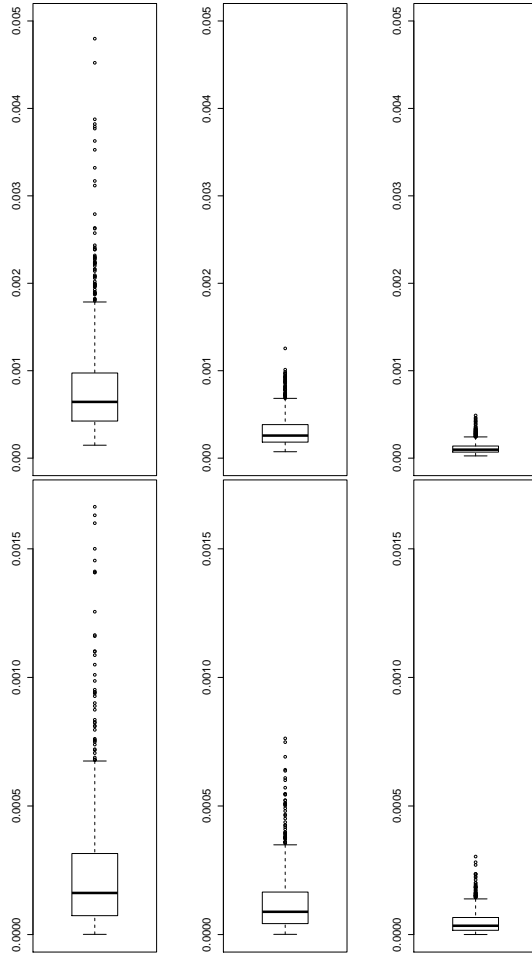


Figure 2: Boxplots of the errors for the conditional shape function estimates ISE_r^F (upper panels) and the conditional intensity factors ISE_r^T (lower panels), in the simulation setting for $n = 100$ (left), $n = 200$ (middle) and $n = 500$ (right).

6. Data Applications and Extensions

6.1 Chicago's Divvy Bike System

We illustrate our approach for the bike trips records of the Chicago Divvy bike system, which is publicly available at <https://www.divvybikes.com/system-data>. The bike trip records contain information such as the bike pickup and drop-off location, date and time, between more than 600 bike rental stations in Chicago. In the context of replicated temporal Poisson processes, [Gervini and Khanal \(2019\)](#) analyzed this dataset by adapting an additive principal component model to the log-intensity functions of daily pickups and estimating

model parameters through a likelihood based approach. Bike sharing systems like the Divvy system in Chicago have been extensively studied (Borgnat et al. 2011). We considered the point process of daily pickups of bikes in a cluster consisting of 6 stations not far from each other in the Chicago Divvy system during weekdays of 2017 (see Figure 3). For bike trips that originated from one of these stations, we obtained the pickup time and counted how many pick-ups occurred in the time window $[0, t)$, $t \in [0, 24]$ hours, to construct the point process. It is of interest to study how temperature affects the intensity function of bike pickups. For this purpose, we employed the local regression approach where the replications of the point process correspond to each weekday (Monday-Friday) during 2017, excluding holidays.

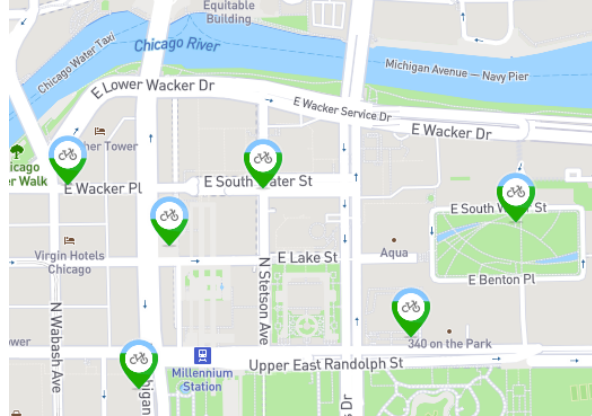


Figure 3: Six bike stations in Chicago, north of E Randolph St and east of N Wabash Ave.

To study the effect of the temperature on the demand of bikes, we obtained the daily observed temperature in Chicago as recorded at the weather station 'Northerly island' from <https://www.ncdc.noaa.gov> and fitted a local Fréchet regression model to obtain the conditional intensity functions of the bike rentals, using estimates $\hat{\Lambda}_\oplus(x)$ as in (11), where we used a bandwidth of 1.5°C . The results are presented in Figure 4.

We observe a clear difference between days with temperature above 10°C which have a uniformly higher intensity function compared to days with lower temperature. In both cases, the shape of the intensity function appears to be bimodal with peaks at 9am and 5pm, which are likely due to bike rentals for the purpose of commuting to the workplace. Moreover, the conditional intensity function estimate is higher around 5pm compared to the early peak

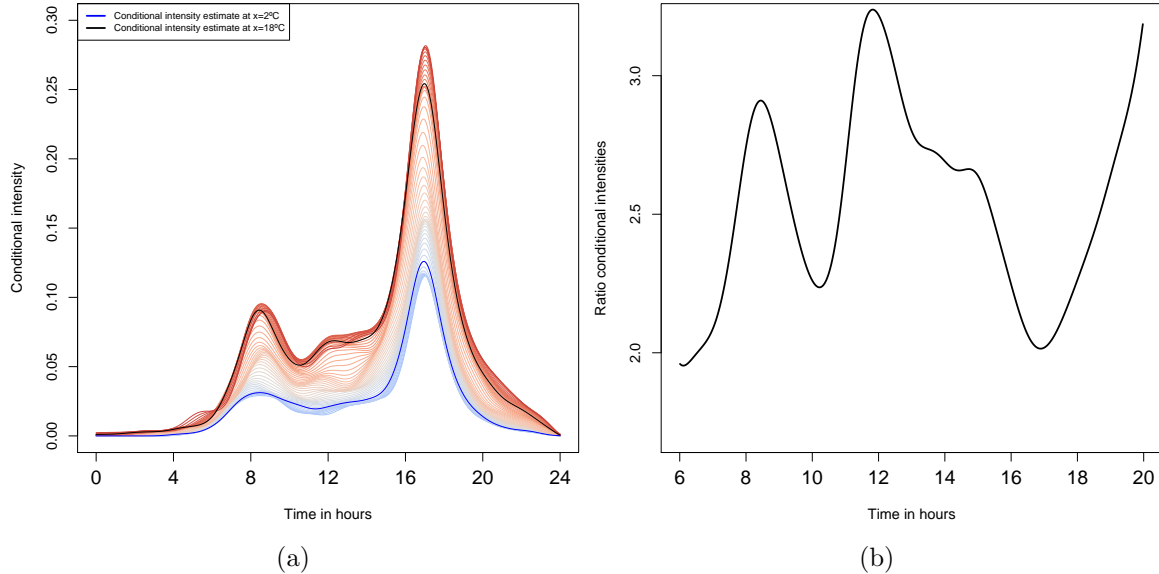


Figure 4: (a) Estimated conditional intensity functions in dependence on temperature values between -2°C (blue) and 24°C (red), using bandwidth $h = 1.5^\circ\text{C}$, with highlighted conditional intensity functions at temperatures 2°C and 18°C . (b) Ratio between the estimated conditional intensity functions at temperature 18°C to that at 2°C .

at 9am, which may be explained by the fact that it is warmer and easier to bike in the afternoon than early in the morning, so perhaps commuters use public or shared transport in the morning and a bike in the afternoon.

There appears to be a “shoulder” or minor peak of bike rental demand at around 12pm on warm days only, which is likely related to more or less optional lunch break related bicycle travel, for leisure or to catch some food. Overall, we find that increasing temperature boosts the bike rental demand in this region of Chicago. Figure 4 (b) shows the quotient between the estimated conditional intensity function at $x = 2^\circ\text{C}$ and $x = 18^\circ\text{C}$. We observe that the ratio is much higher around noon compared to the ratios at 9am and 5 pm. This suggests a change in shape related to temperature; moreover, this ratio is higher for the morning commute compared to the evening commute, indicating that the afternoon demand is not just a reflection of the morning demand. This ratio can be characterized as the degree to which bike travel is optional, where the obvious alternatives to making a trip by bike are not making a trip or making the trip by other means of transportation.

6.2 New York Yellow Taxi System

The New York yellow taxi trip records is a rich and large scale database that contains information such as the taxi pickup and drop-off latitude and longitude locations as well as the date and time, among several other variables. The data is available from the NYC Taxi and Limousine Commission (TLC) at http://www.nyc.gov/html/tlc/html/about/trip_record_data.shtml. Using point processes, this data has been studied by several authors in an applied setting; see for example [Sayarshad and Chow \(2016\)](#) and the references therein for a review and comparison of different intensity models. The Poisson process as a working model for the taxi pickups at a fixed location is well justified theoretically as a superposition of many independent and sufficiently sparse point processes, similar to the case of call arrivals at a telephone exchange ([Cox and Isham 1980](#)). It is of interest to study how the demand of taxis is associated with the day of the week and for this we employ a regression approach.

We consider the point process of daily pickups of yellow taxis that occurred at Penn station in Manhattan during 2017. Penn station is a major train station located in Midtown Manhattan that serves commuters from New York City, New Jersey and Long Island, and connects NYC with several other cities. We view these data as a sample of replicated point processes, as each day produces a replication of the underlying data generation mechanism. To study the effect of weekdays and weekends on the demand of taxis at Penn station, we consider a categorical predictor X that indicates whether the day corresponds to a Monday–Thursday, Friday, Saturday or Sunday. Since local smoothing does not apply to indicator type predictors, we instead consider a global regression framework that is well suited for categorical predictors and is introduced in section 6.3 below, along with convergence results.

Fitting a global regression model for the intensity function on the day of week X by using the estimates $\hat{\Lambda}_{G\oplus}(x)$ defined after Theorem 4 leads to the results as presented in Figure 5. For Sundays, the intensity function is highest late in the day and after 4pm is higher than on all other days, likely due to people returning to New York City from a trip to outside of town. The weekday (Monday through Thursday) intensity function is bimodal with a higher first mode. These modes likely correspond to the commuter traffic, where the 8am mode would be due to commuters who live outside New York City and arrive for work in the City in the morning, while the evening mode likely corresponds to people who return from out

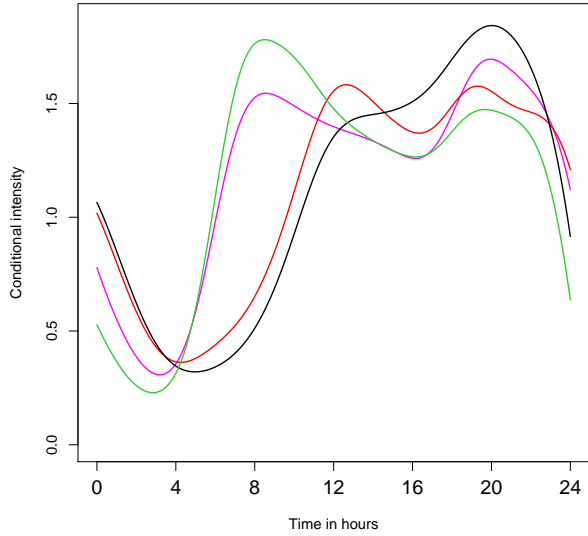


Figure 5: Estimated intensity functions using global regression with type of day as predictors. The fitted response functions are shown for Monday-Thursday (green), Friday (magenta), Saturday (orange) and Sunday (black). The Y-axis is scaled by a factor of 10^{-5} .

of town at Penn Station and hail a taxi there. On Fridays, the same modes are present but with a reversal of their height, as the second mode is now higher than the first mode, likely corresponding to reverse commuters who live in New York City and return from outside, perhaps having a work place away from the City. The patterns for Saturday are also bimodal but with different locations and levels of the modes, indicating that relative large numbers of people arrive at Penn Station around noon and at 8pm, perhaps indicating leisure and shopping trips.

6.3 Global Regression Framework for Intensity Functions

Since the New York taxi data analysis involved indicator variables as predictors for which the previously studied local regression approaches are not applicable, we briefly demonstrate here a generalization of multiple linear regression to the case where responses are point processes that allows the inclusion of categorical predictors while responses are objects residing in intensity space (Ω, d) . The key is a characterization of multiple linear regression as a weighted sum of the responses, which can then be generalized to the case of weighted Fréchet means (Petersen and Müller 2019).

For this, consider an Euclidean predictor $X \in \mathbb{R}^p$ and assume that $\mu := EX$ and $\Sigma :=$

$\text{Var}(X)$ exist, with Σ positive definite. The standard linear regression setting for $(X, \tilde{Y}) \in \mathbb{R}^p \times \mathbb{R}$ is that the regression function $E(\tilde{Y}|X = x) = \beta_0 + \beta_1^T(x - \mu)$ is linear in x , where β_0 and β_1 are the scalar intercept and slope vector, respectively. Petersen and Müller (2019) recharacterized the linear regression function as $E(\tilde{Y}|X = x) = \arg \min_{y \in \mathbb{R}} E(s(X, x)d_E^2(\tilde{Y}, y))$, where $s(X, x) := 1 + (X - \mu)^T \Sigma^{-1}(x - \mu)$ are weights that vary with x and d_E is the Euclidean metric. This allows a direct generalization to linear regression in intensity space (Ω, d) by simply replacing \tilde{Y} to the object $Y \in \Omega$ and the standard Euclidean distance d_E by the metric d in intensity space, which inherits properties of the standard linear regression setup as we show below.

The global regression function of $Y \in \Omega$ on X is given by

$$m_{G\oplus}(x) := \arg \min_{w \in \Omega} E(s(X, x)d^2(Y, w)).$$

Although Ω is not a linear space due to the non-negative nature of the intensity functions, the global regression curve $m_{G\oplus}(x)$ passes through the Fréchet mean of Y at $x = \mu$ since $s(X, \mu) = 1$, a feature inherent to linear regression models. Moreover, the weights $s(X, x)$ can be negative and do not necessarily decay to zero away from x and do not depend on a tuning parameter like local methods do. Similar arguments to the ones outlined in section 3.1 show that $m_{G\oplus}(x) = (\tau_{G\oplus}(x), f_{G\oplus}(x))$, where

$$\tau_{G\oplus}(x) = \arg \inf_{\tau_0 \in \Omega_{\mathcal{T}}} E(s(X, x)d_{\mathcal{T}}^2(\tau, \tau_0)) = \max\{E(s(X, x)\tau), 0\}; \quad (12)$$

$$f_{G\oplus}(x) = \arg \inf_{f_0 \in \Omega_{\mathcal{F}}} E(s(X, x)d_{\mathcal{F}}^2(f, f_0)). \quad (13)$$

Suppose that a sample of replicates $(X_i, N_i, f_i, \tau_i) \stackrel{iid}{\sim} (X, N, f, \tau)$, where $N|\Lambda = f \times \tau$ is a Poisson process with intensity function $\lambda = f \times \tau$, is available and consider the same asymptotic framework as outlined in section 4.1. To obtain empirical estimates, define $s_{in}(x) := 1 + (X_i - \bar{X})^T \hat{\Sigma}^{-1}(x - \bar{X})$, where $\bar{X} := n^{-1} \sum_{i=1}^n X_i$ and $\hat{\Sigma} := n^{-1} \sum_{i=1}^n (X_i - \bar{X})(X_i - \bar{X})^T$. The next result shows that the global regression function in $\Omega_{\mathcal{T}}$ space, $\tau_{G\oplus}(x)$, can be consistently estimated up to the constant $E(\tau)$.

Theorem 3. *Suppose that $1 \leq \tau \leq M_1$ for some constant $M_1 \in [1, \infty)$, $\alpha_n = O(n)$ and $\alpha_n/\log n \rightarrow \infty$ as $n \rightarrow \infty$. Then*

$$\max \left(0, \frac{n^{-1} \sum_{i=1}^n s_{in}(x) N_i(T)}{\bar{N}(T)} \right) = \frac{1}{E(\tau)} \tau_{G\oplus}(x) + O_p(\alpha_n^{-1/2}).$$

Theorem 3 shows that faster rates of convergence can be obtained compared to the local setting, as the sequence α_n is less restricted. The fastest rate achievable is the \sqrt{n} -rate and occurs when the sequence $\alpha_n/n \rightarrow C$ for some $C > 0$, as $n \rightarrow \infty$.

Similarly as in the local regression setup, the shape components f_i remain unobserved and must be estimated from the arrival times across each replication. We consider the same estimation scheme for the shape functions as outlined in section 3.2 but replacing the local weights $s_{in}(x, h)$ by the global weights $s_{in}(x)$. Thus, we have available the empirical estimate $\tilde{f}_{G\oplus}(x)$ of $f_{G\oplus}(x)$. The following result shows consistency of the estimated global regression function in $\Omega_{\mathcal{F}}$ space.

Theorem 4. *Suppose that (S1) and (S2) hold, $\tau \geq 1$ and $\frac{\alpha_n}{\log n} \rightarrow \infty$ as $n \rightarrow \infty$. Then*

$$d_{\mathcal{F}}(f_{G\oplus}(x), \tilde{f}_{G\oplus}(x)) = O_p(n^{-1/2} + \alpha_n^{-1/4}).$$

Thus, if α_n has a polynomial growth rate $\alpha_n/n^\rho \rightarrow C$ as $n \rightarrow \infty$ for some $\rho > 0$ and $C > 0$, we obtain the \sqrt{n} -rate as long as $\rho \geq 2$. If $\rho \in (0, 2)$, then the rate achieved is $O_p(n^{-\rho/4})$. The following corollary summarizes the consistency, up to the constant $E(\tau)$, of the empirical estimate $\hat{\Lambda}_{G\oplus}(x) := \max \left(0, \frac{n^{-1} \sum_{i=1}^n s_{in}(x) N_i(T)}{N(T)} \right) \tilde{f}_{G\oplus}(x)$ of the global regression function $m_{G\oplus}(x)$.

Corollary 2. *Under the regularity conditions of Theorems 3 and 4, the estimate $\hat{\Lambda}_{G\oplus}(x)$ of the conditional intensity function $m_{G\oplus}(x)$ is consistent up to the constant $E(\tau)$ in the sense that*

$$d(m_{G\oplus}(x), E(\tau) \hat{\Lambda}_{G\oplus}(x)) = O_p(\alpha_n^{-1/4}),$$

where $\frac{\alpha_n}{\log n} \rightarrow \infty$ and $\alpha_n = O(n)$ as $n \rightarrow \infty$.

Thus, the optimal rate achieved is $O_p(n^{-1/4})$ when $\alpha_n/n \rightarrow C$ for some $C > 0$, which is due to the growth constraint of the sequence α_n from the intensity factor part of the global regression function.

7. Discussion

We develop here a novel fully non-parametric regression method that features point processes as responses coupled with Euclidean predictors $X \in \mathbb{R}^p$ by establishing a connection to conditional barycenters. Crucially, our model is based on the availability of repeated realizations

of the same point process. The random objects for which we construct conditional barycenters are the intensity functions of Cox process which we can represent as taking values in a product metric space. A novelty in point processes is that we are able to achieve consistent estimation of intensity functions (up to a constant scale factor for the intensity that is common to all observed realizations of the point process).

Obtaining such consistency has been an elusive goal and in fact is not possible when one has one realization of the point process over a fixed domain. What we show here is that this completely changes in a regression setting where one can harness concepts of conditional barycenters that have been developed for Fréchet regression. For each point process, one may have a continuous one-dimensional or general vector predictor that is a random variable associated with the point process. In the former case we can use a nonparametric smoothing method under minimal assumptions, while in the latter case we target a global model that is akin to multiple linear regression and makes it possible to include indicators as predictors.

Our approach relies on straightforward computations and does not require the use of functional principal components, a tool that is not well suited for intensity functions as they do not reside in a linear space due to their non-negative nature. We show that the proposed regression model is applicable to many data situations where one is interested in the behavior of point processes in dependence of covariates, including applications in transportation and seismology.

References

Aguech, M. and Carlier, G. (2011), “Barycenters in the Wasserstein space,” *SIAM Journal on Mathematical Analysis*, 43, 904–924.

Bigot, J., Cazelles, E., and Papadakis, N. (2018), “Data-driven regularization of Wasserstein barycenters with an application to multivariate density registration,” *arXiv preprint arXiv:1804.08962*.

Bolstad, B. M., Irizarry, R., Åstrand, M., and Speed, T. (2003), “A comparison of normalization methods for high density oligonucleotide array data based on variance and bias,” *Bioinformatics*, 19, 185–193.

Borgnat, P., Abry, P., Flandrin, P., Robardet, C., Rouquier, J.-B., and Fleury, E. (2011), “Shared bicycles in a city: A signal processing and data analysis perspective,” *Advances in Complex Systems*, 14, 415–438.

Bouzas, P. and Ruiz-Fuentes, N. (2015), “A review on functional data analysis for Cox processes,” *Boletin de Estadistica e Investigacion Operativa*, 215–230.

Bouzas, P. R., Valderrama, M., Aguilera, A. M., and Ruiz-Fuentes, N. (2006), “Modeling the mean of a doubly stochastic Poisson process by functional data analysis,” *Computational Statistics and Data Analysis*, 50, 2655–2667.

Burago, D., Burago, Y., and Ivanov, S. (2001), *A Course in Metric Geometry*, vol. 33, American Mathematical Society.

Cazelles, E., Seguy, V., Bigot, J., Cuturi, M., and Papadakis, N. (2018), “Geodesic PCA versus log-PCA of Histograms in the Wasserstein Space,” *SIAM Journal on Scientific Computing*, 40, B429–B456.

Cox, D. R. and Isham, V. (1980), *Point Processes*, London: Chapman & Hall, monographs on Applied Probability and Statistics.

Cucala, L. (2008), “Intensity estimation for spatial point processes observed with noise,” *Scandinavian Journal of Statistics*, 35, 322–334.

Daley, D. J. and Vere-Jones, D. (2003), *An Introduction to the Theory of Point Processes: volume I: Elementary Theory and Methods, Second Edition*, Springer, New York.

Diggle, P. and Marron, J. (1988), “Equivalence of smoothing parameter selections in density and intensity estimation,” *Journal of the American Statistical Association*, 83, 793–800.

Diggle, P. J. (1985), “A kernel method for smoothing point process data,” *Applied Statistics*, 34, 138–147.

Diggle, P. J., Moraga, P., Rowlingson, B., and Taylor, B. M. (2013), “Spatial and spatio-temporal log-Gaussian Cox processes: extending the geostatistical paradigm,” *Statistical Science*, 28, 542–563.

Fan, J. and Gijbels, I. (1996), *Local Polynomial Modelling and its Applications*, London: Chapman & Hall.

Fan, J., Gijbels, I., Hu, T.-C., and Huang, L.-S. (1996), “A study of variable bandwidth selection for local polynomial regression,” *Statistica Sinica*, 113–127.

Fréchet, M. (1948), “Les éléments aléatoires de nature quelconque dans un espace distancié,” in *Annales de l’Institut Henri Poincaré*, vol. 10, pp. 215–310.

Gervini, D. (2017), “Multiplicative component models for replicated point processes,” *arXiv preprint arXiv:1705.09693*.

Gervini, D. and Khanal, M. (2019), “Exploring patterns of demand in bike sharing systems via replicated point process models,” *Journal of the Royal Statistical Society Series C: Applied Statistics*, 68, 585–602.

Grenander, U. (1950), “Stochastic processes and statistical inference,” *Arkiv för Matematik*, 1, 195–277.

Kleffe, J. (1973), “Principal components of random variables with values in a separable Hilbert space,” *Statistics: A Journal of Theoretical and Applied Statistics*, 4, 391–406.

Lawless, J. F. (1987), “Regression methods for Poisson process data,” *Journal of the American Statistical Association*, 82, 808–815.

Li, Y. and Guan, Y. (2014), “Functional principal component analysis of spatiotemporal point processes with applications in disease surveillance,” *Journal of the American Statistical Association*, 109, 1205–1215.

Mikosch, T. (2009), *Non-Life Insurance Mathematics: An Introduction with the Poisson Process*, Springer.

Panaretos, V. M. and Zemel, Y. (2016), “Amplitude and phase variation of point processes,” *The Annals of Statistics*, 44, 771–812.

Panaretos, V. M. and Zemel, Y. (2019), “Statistical Aspects of Wasserstein Distances,” *Annual Review of Statistics and Its Application*, 6, 405–431.

Petersen, A., Deoni, S., and Müller, H.-G. (2019), “Fréchet estimation of time-varying covariance matrices from sparse data, with application to the regional co-evolution of myelination in the developing brain,” *The Annals of Applied Statistics*, 13, 393–419.

Petersen, A. and Müller, H.-G. (2019), “Fréchet regression for random objects with Euclidean predictors,” *The Annals of Statistics*, 47, 691–719.

Reddy, S. K. and Dass, M. (2006), “Modeling On-Line Art Auction Dynamics Using Functional Data Analysis,” *Statistical Science*, 21, 179–193.

Sayarshad, H. R. and Chow, J. Y. J. (2016), “Survey and empirical evaluation of nonhomogeneous arrival process models with taxi data,” *Journal of Advanced Transportation*, 50, 1275–1294.

Shmueli, G., Russo, R. P., and Jank, W. (2007), “The BARISTA: A model for bid arrivals in online auctions,” *The Annals of Applied Statistics*, 1, 412–441.

Utsu, T., Ogata, Y., S, R., and Matsu’ura (1995), “The centenary of the Omori formula for a decay law of aftershock activity,” *Journal of Physics of the Earth*, 43, 1–33.

Villani, C. (2003), *Topics in Optimal Transportation*, American Mathematical Society.

Wu, S., Müller, H.-G., and Zhang, Z. (2013), “Functional data analysis for point processes with rare events,” *Statistica Sinica*, 23, 1–23.

Zhang, T. and Kou, S. C. (2010), “Nonparametric inference of doubly stochastic Poisson process data via the kernel method,” *The Annals of Applied Statistics*, 4, 1913–1941.

Supplement

S.1 Proofs of Results in Section 4.1

Proof of Lemma 1

Let $Q_1, Q_2 \in Q(\Omega_{\mathcal{F}})$, $\lambda \in [0, 1]$ and $Q_\lambda = \lambda Q_1 + (1 - \lambda)Q_2$ and $x, y \in [0, 1]$. It is clear that $Q_\lambda(0) = 0$, $Q_\lambda(1) = T$, $Q_\lambda(\cdot)$ is strictly increasing and that by the triangle inequality

$|Q_\lambda(x) - Q_\lambda(y)| \leq L|x - y|$. Suppose now that $x \leq y$, then since Q_λ is monotonic we have $|Q_\lambda(x) - Q_\lambda(y)| = Q_\lambda(y) - Q_\lambda(x)$. Furthermore, for M as in (S1),

$$\begin{aligned} Q_\lambda(y) - Q_\lambda(x) &= \lambda(Q_1(y) - Q_1(x)) + (1 - \lambda)(Q_2(y) - Q_2(x)) \\ &\geq \lambda M(y - x) + (1 - \lambda)M(y - x) = M(y - x), \end{aligned}$$

which implies $|Q_\lambda(x) - Q_\lambda(y)| \geq M|x - y|$ for all $x, y \in [0, 1]$. Hence, $Q(\Omega_{\mathcal{F}})$ is convex and it is clearly a subset of $L^2([0, 1])$ since the quantile functions are bounded. Next, let Q_1, Q_2, \dots be a sequence in $Q(\Omega_{\mathcal{F}})$ such that $Q_n \xrightarrow{L^2} Q \in L^2([0, 1])$ as $n \rightarrow \infty$. We show that $Q \in Q(\Omega_{\mathcal{F}})$. In fact, since the family $\{Q_n\}_{n=1}^\infty$ has a common Lipschitz constant L , it follows that it is uniformly equicontinuous. Moreover, since $[0, 1]$ is compact and $Q_n \xrightarrow{L^2} Q \in L^2([0, 1])$ then $Q_n \rightarrow Q$ uniformly as $n \rightarrow \infty$. This implies $Q(0) = 0$, $Q(1) = T$ and that $Q_n(\cdot)$ is non-decreasing. Now, Q must be strictly increasing since otherwise there exist $t_1, t_2 \in [0, 1]$ with $t_1 < t_2$ such that $Q(t_1) = Q(t_2)$, and then, for any $\epsilon > 0$, by uniform convergence we have $\|Q_n - Q\|_\infty \leq \epsilon/2$ for n big enough and furthermore

$$\begin{aligned} M|t_2 - t_1| &\leq |Q_n(t_2) - Q_n(t_1)| \leq |Q_n(t_2) - Q(t_2)| + |Q(t_2) - Q_n(t_1)| \\ &= |Q_n(t_2) - Q(t_2)| + |Q(t_1) - Q_n(t_1)| \leq 2\|Q_n - Q\|_\infty \leq \epsilon, \end{aligned}$$

and choosing ϵ small enough leads to a contradiction. Next, for any $x, y \in [0, 1]$ and $\epsilon > 0$ we have that $\|Q_n - Q\|_\infty \leq \epsilon/2$ for n big enough and

$$\begin{aligned} |Q(x) - Q(y)| &\leq |Q(x) - Q_n(x)| + |Q_n(x) - Q_n(y)| + |Q_n(y) - Q(y)| \\ &\leq 2\|Q_n - Q\|_\infty + L|x - y| \leq \epsilon + L|x - y|, \end{aligned}$$

for large enough $n(\epsilon)$, using that $Q_n \in Q(\Omega_{\mathcal{F}})$ by assumption and the functions in this space satisfy the Lipschitz condition with constant L . Taking $\epsilon \downarrow 0$ we obtain that Q is also Lipschitz with constant L . Similarly,

$$M|x - y| \leq |Q_n(x) - Q_n(y)| \leq 2\|Q_n - Q\|_\infty + |Q(x) - Q(y)| \leq \epsilon + |Q(x) - Q(y)|,$$

so that Q satisfies condition (S1). Therefore, $Q(\Omega_{\mathcal{F}})$ is closed.

Proof of Proposition 1.

From (10) we have

$$d_{\mathcal{F}}(\hat{f}_\oplus(x), \tilde{f}_\oplus(x)) \leq n^{-1} \sum_{i=1}^n |s_{in}(x, h)| \|\hat{Q}_i - Q_i\|_{L^2([0, 1])}.$$

Adopting similar arguments as in the proof of Theorem 1 in [Petersen et al. \(2019\)](#), $|s_{in}(x, h)| = O_p(K_h(X_i - x))$, where the bound is uniform in i . Next, we obtain

$$\|\hat{Q}_i - Q_i\|_{L^2([0,1])} = O_p(\alpha_n^{-1/4}),$$

where the bound is uniform in i , which follows from similar arguments as in the proof of Theorem 2 in [Panaretos and Zemel \(2016\)](#). This implies

$$n^{-1} \sum_{i=1}^n |s_{in}(x, h)| \|\hat{Q}_i - Q_i\|_{L^2([0,1])} = O_p \left(\frac{\alpha_n^{-1/4}}{n} \sum_{i=1}^n K_h(X_i - x) \right) = O_p(\alpha_n^{-1/4}).$$

Proof of Theorem 1.

Under the assumptions $(K0)$, $(L1)$ and $f_X > 0$ with unbounded support and the choice of h_n , we have from [Petersen and Müller \(2019\)](#) that

$$d_{\mathcal{F}}(f_{\oplus}(x), \hat{f}_{\oplus}(x)) = O_p(n^{-2/5})$$

Finally, the result follows by using Proposition 1 and the triangle inequality (9).

S.2 Proof of Results in Section 4.2

We begin by establishing four auxiliary lemmas.

Lemma S.1 *Suppose that $\tau \geq 1$. Then, for all $i = 1, \dots, n$,*

$$\sqrt{\frac{\alpha_n}{\tau_i}} \left(\frac{N_i(T)}{\alpha_n} - \tau_i \right) = O_p(1),$$

where the $O_p(1)$ term is uniform in i .

Proof of Lemma S.1.

Since N_i is a Cox process, it is generated by two independent random mechanisms: First the generation of the intensity function Λ_i , and then, conditional on Λ_i , of the realizations of N_i corresponding to those of a Poisson process $N_i(\cdot | \Lambda_i)$ with intensity function $\alpha_n \Lambda_i$ ([Daley and Vere-Jones 2003](#)). Thus, we may regard the probability space associated with the generation of the intensity function and the Poisson process as a product probability space $\mathcal{W}_1 \times \mathcal{W}_2$ such that $\Lambda_i = \Lambda_i(w_1)$ with $w_1 \in \mathcal{W}_1$ is a realization of the intensity function and then

$N_i(\cdot) = N_i(\cdot, w_2)$ with $w_2 \in \mathcal{W}_2$ is a realization of a Poisson process with intensity function $\alpha_n \Lambda_i$. For $\tau_i := \int_0^T \Lambda_i(s)ds$ and any $M > 0$ we have

$$\begin{aligned} \mathbb{P}(\sqrt{\alpha_n/\tau_i} |N_i(T)/\alpha_n - \tau_i| > M) &= E_{\mathcal{W}_1}[\mathbb{P}_{\mathcal{W}_2}(|N_i(T)/\alpha_n - \tau_i| > M\sqrt{\tau_i/\alpha_n} |\Lambda_i(w_1)))] \\ &\leq E_{\mathcal{W}_1}[(\alpha_n/(M^2\tau_i))\text{Var}_{\mathcal{W}_2}(N_i(T)/\alpha_n |\Lambda_i(w_1))] = 1/M^2, \end{aligned}$$

where the last equality follows from the fact that given $\Lambda_i(w_1)$, we have $N_i(T) \sim \mathcal{P}(\alpha_n \tau_i(w_1))$, with (conditional) variance $\alpha_n \tau_i(w_1)$. Hence, for any $\epsilon > 0$ we can choose M large enough and independent of i such that $\mathbb{P}(\sqrt{\alpha_n/\tau_i} |N_i^{(n)}(T)/\alpha_n - \tau_i| > M) < \epsilon$.

Lemma S.2 *If there exists $M_1 < \infty$ such that $1 \leq \tau \leq M_1$, then*

$$\sqrt{\alpha_n} n^{-1} \sum_{i=1}^n s_{in}(x, h) \left(\frac{N_i(T)}{\alpha_n} - \tau_i \right) = O_p(1).$$

Proof of Lemma S.2.

Observing

$$\sqrt{\alpha_n} n^{-1} \sum_{i=1}^n s_{in}(x, h) \left(\frac{N_i(T)}{\alpha_n} - \tau_i \right) = n^{-1} \sum_{i=1}^n s_{in}(x, h) \sqrt{\frac{\alpha_n}{\tau_i}} \left(\frac{N_i(T)}{\alpha_n} - \tau_i \right) \sqrt{\tau_i},$$

and applying Lemma S.1 and the fact that τ_i is uniformly bounded above, we have $\sqrt{\alpha_n/\tau_i}(N_i(T)/\alpha_n - \tau_i)\sqrt{\tau_i} = O_p(1)$ uniformly in i . By the same arguments as in the proof of Theorem 1 in Petersen et al. (2019), it follows that $|s_{in}(x, h)| = O_p(K_h(X_i - x))$ uniformly in i and

$$\begin{aligned} n^{-1} \sum_{i=1}^n s_{in}(x, h) \sqrt{\frac{\alpha_n}{\tau_i}} \left(\frac{N_i(T)}{\alpha_n} - \tau_i \right) \sqrt{\tau_i} &\leq n^{-1} \sum_{i=1}^n |s_{in}(x, h)| \left| \sqrt{\frac{\alpha_n}{\tau_i}} \left(\frac{N_i(T)}{\alpha_n} - \tau_i \right) \sqrt{\tau_i} \right| \\ &= O_p \left(n^{-1} \sum_{i=1}^n K_h(X_i - x) \right) = O_p(1). \end{aligned}$$

For the following, recall that $\bar{N}(T) := n^{-1} \sum_{i=1}^n N_i(T)$.

Lemma S.3 *If $1 \leq \tau \leq M_1$ and $\alpha_n \rightarrow \infty$ as $n \rightarrow \infty$, then*

$$\sqrt{n} \left(\frac{\bar{N}(T)}{\alpha_n} - E(\tau) \right) = O_p(1). \quad (14)$$

Proof of Lemma S.3.

The result follows from an application of a central limit theorem for triangular arrays. Let $a_i = N_i(T)/\alpha_n$, then by conditioning on Λ_i it follows that $E(a_i) = E(\tau)$ and $\sigma_i^2 := \text{Var}(a_i) = \text{Var}(\tau) + E(\tau)/\alpha_n$. Setting $s_n^2 = \sum_{i=1}^n \sigma_i^2 = n(\text{Var}(\tau) + E(\tau)/\alpha_n)$, we show that

$$\frac{1}{s_n} \sum_{i=1}^n a_i - E(\tau) \xrightarrow{\mathcal{L}} N(0, 1), \quad (15)$$

whence we may infer $\sqrt{n} \left(\frac{\bar{N}(T)}{\alpha_n} - E(\tau) \right) / \sqrt{\text{Var}(\tau) + E(\tau)/\alpha_n} = O_p(1)$ and furthermore (14), since $\text{Var}(\tau) + E(\tau)/\alpha_n$ is bounded above as τ is uniformly bounded and the positive sequence α_n satisfies $1/\alpha_n \rightarrow 0$ as $n \rightarrow \infty$. The Lyapunov condition

$$\lim_{n \rightarrow \infty} \frac{1}{s_n^4} \sum_{i=1}^n E(N_i(T)/\alpha_n - E(\tau))^4 = 0 \quad (16)$$

implies (15) and will hold if we show $\lim_{n \rightarrow \infty} \frac{1}{n\alpha_n^4} E(N_1(T) - \alpha_n E(\tau))^4 = 0$. Noting that $N_1(T)|\Lambda_1 \sim \mathcal{P}(\alpha_n \tau_1)$ and

$$(N_1(T) - \alpha_n E(\tau))^4 = N_1(T)^4 - 4N_1(T)^3 \alpha_n E(\tau) + 6N_1(T)^2 \alpha_n^2 E(\tau)^2 - 4N_1(T) \alpha_n^3 E(\tau)^3 + \alpha_n^4 E(\tau)^4, \quad (17)$$

conditional on Λ_1 , the higher order moments of $N_1(T)|\Lambda_1$ are given by $E(N_1(T)^4|\Lambda_1) = (\alpha_n \tau_1)^4 + 6(\alpha_n \tau_1)^3 + 7(\alpha_n \tau_1)^2 + (\alpha_n \tau_1)$, $E(N_1(T)^3|\Lambda_1) = (\alpha_n \tau_1)^3 + 3(\alpha_n \tau_1)^2 + (\alpha_n \tau_1)$ and $E(N_1(T)^2|\Lambda_1) = (\alpha_n \tau_1)^2 + (\alpha_n \tau_1)$. Finally, by taking expectation of the conditional moments and using the fact that τ_1 is uniformly bounded along with equation (17) leads to $\lim_{n \rightarrow \infty} \frac{1}{n\alpha_n^4} E(N_1(T) - \alpha_n E(\tau))^4 = 0$, completing the proof.

Lemma S.4 Suppose that $\alpha_n = O(n^{4/5})$ and $\frac{\alpha_n}{\log n} \rightarrow \infty$ as $n \rightarrow \infty$, and $1 \leq \tau \leq M_1$. Then

$$\sqrt{\alpha_n} (\bar{N}(T)/\alpha_n)^{-1} E(\tau|X=x) = \sqrt{\alpha_n} E(\tau|X=x)/E(\tau) + O_p(1). \quad (18)$$

Proof of Lemma S.4.

From Lemma S.3 we have $\bar{N}(T)/\alpha_n = E(\tau) + O_p(n^{-1/2})$, and a Taylor expansion leads to

$$(\bar{N}(T)/\alpha_n)^{-1} = \frac{1}{E(\tau)} - \frac{1}{E(\tau)^2} \left(\frac{\bar{N}(T)}{\alpha_n} - E(\tau) \right) + o_p(n^{-1/2}).$$

With $m(x) = E(\tau|X = x)$ one obtains

$$\sqrt{\alpha_n}(\bar{N}(T)/\alpha_n)^{-1}m(x) = \frac{\sqrt{\alpha_n}}{E(\tau)}m(x) - \frac{m(x)}{E(\tau)^2}\frac{\sqrt{\alpha_n}}{\sqrt{n}}\sqrt{n}\left(\frac{\bar{N}(T)}{\alpha_n} - E(\tau)\right) + o_p\left(\sqrt{\alpha_n/n}\right).$$

The results follows since $\alpha_n = O(n^{4/5})$ implies $\alpha_n/n \rightarrow 0$ as $n \rightarrow \infty$ and by using Lemma S.3.

Proof of Theorem 2.

In effect

$$\begin{aligned} & \sqrt{\alpha_n} \frac{n^{-1} \sum_{i=1}^n s_{in}(x, h) N_i(T)}{\bar{N}(T)} \\ &= \sqrt{\alpha_n}(\bar{N}(T)/\alpha_n)^{-1} n^{-1} \sum_{i=1}^n s_{in}(x, h)(N_i(T)/\alpha_n - \tau_i) + \sqrt{\alpha_n}(\bar{N}(T)/\alpha_n)^{-1} n^{-1} \sum_{i=1}^n s_{in}(x, h) \tau_i \\ &= (\bar{N}(T)/\alpha_n)^{-1} O_p(1) + (\sqrt{\alpha_n}/n^{2/5})(\bar{N}(T)/\alpha_n)^{-1}(n^{2/5}E(\tau|X = x) + O_p(1)) \\ &= (\bar{N}(T)/\alpha_n)^{-1} O_p(1) + \sqrt{\alpha_n}(\bar{N}(T)/\alpha_n)^{-1} E(\tau|X = x) + (\bar{N}(T)/\alpha_n)^{-1} O_p(1) \\ &= \sqrt{\alpha_n} \frac{E(\tau|X = x)}{E(\tau)} + O_p(1), \end{aligned}$$

where the second equality follows from Lemma S.2 and by applying Lemma S.5 below with $h = h_n \sim c_0 n^{-1/5}$ for some constant $c_0 > 0$; and the last equality follows from Lemma S.4.

The result follows.

S.3 Consistency of Local Linear Estimator

In this section we show only for completeness the well known result regarding the asymptotic normality of the local linear regression estimate for the conditional mean function. Suppose that $(X_1, Y_1), \dots, (X_n, Y_n) \stackrel{iid}{\sim} (X, Y)$ where X and Y are real valued. Let $m(x) = E(Y|X = x)$ be the regression function and $f(x) > 0$ be the design density function. Then, the local linear regression estimate (Fan and Gijbels 1996) $\hat{m}(x)$ of $m(x)$ is given by

$$\hat{m}(x) = b_1^T \left(\frac{1}{n} \mathbf{X}^T \mathbf{W} \mathbf{X} \right)^{-1} \left(\frac{1}{n} \mathbf{X}^T \mathbf{W} \mathbf{Y} \right), \quad b_1 = (1 \ 0)^T,$$

where $\mathbf{W} = \text{diag}(K_h(X_i - x))$, $K_h(\cdot) = K(\cdot)/h$ with $K(\cdot)$ a kernel function, $\mathbf{Y} = (Y_1, \dots, Y_n)^T$, and the i^{th} row of \mathbf{X} is given by $(1, X_i - x)$, $i = 1, \dots, n$. Now, if we let $\hat{u}_j := n^{-1} \sum_{i=1}^n K_h(X_i - x)(X_i - x)^j$ and $\hat{\sigma}_0^2 := \hat{u}_0 \hat{u}_2 - \hat{u}_1^2$, it can be checked that

$$\left(\frac{1}{n} \mathbf{X}^T \mathbf{W} \mathbf{X} \right)^{-1} = \begin{bmatrix} \frac{\hat{u}_2}{\hat{\sigma}_0^2} & -\frac{\hat{u}_1}{\hat{\sigma}_0^2} \\ -\frac{\hat{u}_1}{\hat{\sigma}_0^2} & \frac{\hat{u}_0}{\hat{\sigma}_0^2} \end{bmatrix}$$

and

$$\frac{1}{n} \mathbf{X}^T \mathbf{W} \mathbf{Y} = \begin{bmatrix} n^{-1} \sum_{i=1}^n K_h(X_i - x) Y_i \\ n^{-1} \sum_{i=1}^n K_h(X_i - x)(X_i - x) Y_i \end{bmatrix},$$

whence

$$\hat{m}(x) = \begin{bmatrix} \hat{u}_2 \\ \hat{\sigma}_0^2 \end{bmatrix} \begin{bmatrix} n^{-1} \sum_{i=1}^n K_h(X_i - x) Y_i \\ n^{-1} \sum_{i=1}^n K_h(X_i - x)(X_i - x) Y_i \end{bmatrix}. \quad (19)$$

We make the following assumptions:

- (A1) The regression function $m(x) = E(Y|X = x)$, the design density function $f(x) > 0$ and $\sigma^2(x) = E(e^2|X = x)$, where $e = Y - m(X)$, are twice continuously differentiable.
- (A2) The kernel $K(\cdot)$ is bounded and corresponds to a density function which is symmetric around zero and has compact support $[-1, 1]$.
- (A3) As $n \rightarrow \infty$, $nh^5 = O(1)$.
- (A4) There exists $\delta > 0$ and $\bar{\sigma} > 0$ such that $E(|e_i|^{2+\delta}|X_i) \leq \bar{\sigma}$, $i = 1, \dots, n$, where $e_i := Y_i - m(X_i)$.

Note that assumption (A3) implies that as $n \rightarrow \infty$ we have $h \rightarrow 0$, $nh^q \rightarrow \infty$ for $q \in \{0, 1, 2, 3, 4\}$ and $nh^p \rightarrow 0$ for $p \geq 6$ integer.

By a second order Taylor expansion of $m(\cdot)$ around x ,

$$Y_i = m(X_i) + e_i = m(x) + m'(x)(X_i - x) + \frac{m''(x)}{2}(X_i - x)^2 + \frac{(m''(\xi(X_i, x)) - m''(x))}{2}(X_i - x)^2 + e_i,$$

where $\xi(X_i, x)$ lies between x and X_i . By replacing the previous expression in (19) and after some algebra we obtain

$$\hat{m}(x) = m(x) + \begin{bmatrix} \hat{u}_2 \\ \hat{\sigma}_0^2 \end{bmatrix} \begin{bmatrix} \hat{u}_2 \frac{m''(x)}{2} + n^{-1} \sum_{i=1}^n K_h(X_i - x) e_i + R_1 \\ \hat{u}_3 \frac{m''(x)}{2} + n^{-1} \sum_{i=1}^n K_h(X_i - x)(X_i - x) e_i + R_2 \end{bmatrix}, \quad (20)$$

where the remainder terms are given by

$$\begin{aligned} R_1 &= n^{-1} \sum_{i=1}^n K_h(X_i - x) \frac{(m''(\xi(X_i, x)) - m''(x))}{2} (X_i - x)^2, \\ R_2 &= n^{-1} \sum_{i=1}^n K_h(X_i - x) \frac{(m''(\xi(X_i, x)) - m''(x))}{2} (X_i - x)^3. \end{aligned}$$

We now study the asymptotic distribution of $\hat{m}(x)$ with a suitably chosen scaling factor. For this, we introduce the following quantities. Let i, j be non-negative integers and define $k_{ij} := \int_{-1}^1 K(u)^i u^j du$. The auxiliary lemma on the asymptotic normality of $\hat{m}(x)$ is listed for completeness only. Its proof follows by standard arguments. See for example Theorem 5.2 in [Fan and Gijbels \(1996\)](#) and the references therein.

Lemma S.5 *Under assumptions (A1) – (A4),*

$$\sqrt{nh} \left(\hat{m}(x) - m(x) - h^2 \frac{m''(x)}{2} k_{12} \right) \xrightarrow{\mathcal{L}} N \left(0, k_{20} \frac{\sigma^2(x)}{f(x)} \right).$$

as $n \rightarrow \infty$.

5.4 Proofs of Results in Section 6.3

Proof of Theorem 3.

Consider the auxiliary quantities $s_i(x) := 1 + (X_i - \mu)^T \Sigma^{-1}(x - \mu)$, $W_{0n}(x) := \bar{X}^T \Sigma^{-1}(x - \bar{X}) - \mu^T \Sigma^{-1}(x - \mu)$ and $W_{1n}(x) := \Sigma^{-1}(x - \mu) - \hat{\Sigma}^{-1}(x - \bar{X})$. The arguments in the proof of Theorem 1 in [Petersen and Müller \(2019\)](#) show that $W_{0n} = O_p(n^{-1/2})$, $\|W_{1n}\|_2 = O_p(n^{-1/2})$ and $s_{in}(x) - s_i(x) = -W_{0n} - W_{1n}^T X_i$. Thus

$$\begin{aligned} n^{-1} \sum_{i=1}^n s_{in}(x) N_i(T) / \alpha_n \\ = -W_{0n} \bar{N}(T) / \alpha_n - n^{-1} \sum_{i=1}^n X_i^T (N_i(T) / \alpha_n) W_{1n} + n^{-1} \sum_{i=1}^n s_i(x) N_i(T) / \alpha_n. \end{aligned} \quad (21)$$

Next, note that $W_{0n} \bar{N}(T) / \alpha_n = W_{0n} (\bar{N}(T) / \alpha_n - E(\tau)) + W_{0n} E(\tau) = O_p(n^{-1/2})$ by Lemma S.3. Further, from the fact that $E(\|X_1\|_2 N_1(T) / \alpha_n) \leq (E\|X_1\|_2^2 E(N_1(T) / \alpha_n)^2)^{1/2} = \sqrt{(tr(\Sigma) + \|\mu\|_2^2)(E(\tau^2) + o(1))}$ is uniformly bounded and the inequality $\|n^{-1} \sum_{i=1}^n X_i^T (N_i(T) / \alpha_n)\|_2 \leq n^{-1} \sum_{i=1}^n (N_i(T) / \alpha_n) \|X_i\|_2$, it follows that $n^{-1} \sum_{i=1}^n X_i^T (N_i(T) / \alpha_n) = O_p(1)$ and thus $n^{-1} \sum_{i=1}^n X_i^T (N_i(T) / \alpha_n) W_{1n} = O_p(n^{-1/2})$. This shows that

$$n^{-1} \sum_{i=1}^n s_{in}(x) N_i(T) / \alpha_n = n^{-1} \sum_{i=1}^n s_i(x) N_i(T) / \alpha_n + O_p(n^{-1/2}). \quad (22)$$

Next, note that

$$n^{-1} \sum_{i=1}^n s_i(x) N_i(T) / \alpha_n = n^{-1} \sum_{i=1}^n s_i(x) (N_i(T) / \alpha_n - \tau_i) + n^{-1} \sum_{i=1}^n s_i(x) \tau_i$$

$$= n^{-1} \sum_{i=1}^n s_i(x)(N_i(T)/\alpha_n - \tau_i) + E(s(X, x)\tau) + O_p(n^{-1/2}),$$

where the second equality follows from the central limit theorem. Now, from Lemma S.1 and since $s_i(x) = O_p(1)$, where the $O_p(1)$ term is uniform in i , we have

$$\sqrt{\alpha_n} |n^{-1} \sum_{i=1}^n s_i(x)(N_i(T)/\alpha_n - \tau_i)| \leq n^{-1} \sum_{i=1}^n |s_i(x)| \sqrt{\alpha_n/\tau_i} |N_i(T)/\alpha_n - \tau_i| M_1 = O_p(1),$$

so that by using (21), (22) and the condition $\alpha_n = O(n)$ we obtain

$$\sqrt{\alpha_n} n^{-1} \sum_{i=1}^n s_{in}(x) N_i(T)/\alpha_n = \sqrt{\alpha_n} E(s(X, x)\tau) + O_p(1).$$

Finally, similar arguments as the ones outlined in the proof of Lemma S.4 lead to

$$\sqrt{\alpha_n} \frac{n^{-1} \sum_{i=1}^n s_{in}(x) N_i(T)}{\bar{N}(T)} = \sqrt{\alpha_n} \frac{E(s(X, x)\tau)}{E\tau} + O_p(1)$$

and the result follows.

Proof of Theorem 4.

The proof follows by similar arguments as the ones outlined in the proof of Proposition 1 and Theorem 2 in [Petersen and Müller \(2019\)](#), and is therefore omitted.

S.5 Implementation of Local Regression for Intensity Functions

The minimization problem in (8) is solved numerically and similar to the quadratic optimization problem considered in [Petersen and Müller \(2019\)](#). Recall that

$$\tilde{Q}_\oplus(\cdot, x) := \arg \min_{q \in Q(\Omega_F)} \|q - n^{-1} \sum_{i=1}^n s_{in}(x, h) \hat{Q}_i\|_{L^2([0,1])}^2.$$

Let $r_j, j = 1, \dots, \nu$, be an equispaced grid in $(0, 1)$ and define $w_j := n^{-1} \sum_{i=1}^n s_{in}(x, h) \hat{Q}_i(r_j)$, $j = 1, \dots, \nu$. We compute

$$q^* := \arg \min_{q \in \mathbb{R}^\nu} \|q - w\|_E^2,$$

subject to the constraints $q_1 \leq \dots \leq q_\nu$ and $M\Delta r \leq q_{j+1} - q_j \leq L\Delta r$, $j = 1, \dots, \nu - 1$, where $w = (w_1, \dots, w_\nu)^T$, $\Delta r := r_2 - r_1$ is the grid spacing, and M, L , in practice, are taken as very small/large constants, $M = 10^{-10}$ and $L = 10^{10}$. The optimization problem is a quadratic program with linear constraints and can be solved using state of the art optimization routines. The optimal solution q^* corresponds to a discretized version of $\tilde{Q}_\oplus(\cdot, x)$ which is then mapped

back to density space to obtain a discrete approximation of the corresponding density function $\tilde{f}_\oplus(\cdot, x)$. The latter step is performed by first constructing the cdf associated with q^* and then utilizing local linear smoothing methods (Fan et al. 1996). The implementation of the global regression is similar.

S.6 Aftershock Earthquake Process in Chile

We present here another example from seismology, where earthquakes naturally form point processes. So it is not surprising that earthquake activity has met with major interest in the point process literature (Daley and Vere-Jones 2003). Chile is widely known for its strong seismic activity both in intensity and in frequency. Our goal is to study the aftershock process that follows a major earthquake occurring at time $t = 0$, referred to as the mainshock. We focus on the arrival of aftershocks that occur in a time window of 2 months after the mainshock and we suppose $N(t)$ is observed in $[0, T]$ for $T = 2$ months.

To demonstrate our methods, we considered the mainshocks that occurred between 1980 and 2017 in Chile, which include some strong earthquakes such as the magnitude 8.8 earthquake on the moment magnitude scale in February 2010, 8.2 in April 2014, 8.0 in March 1985, and other strong earthquakes. The data was obtained from the U.S. Geological Survey web page <https://earthquake.usgs.gov/earthquakes/search/> which provides information concerning the location, magnitude and date of the earthquakes. We classified each earthquake in terms of its magnitude category and selected 15 mainshocks at random from each category in the order strongest to weakest. This enables us to consider the strongest earthquakes above magnitude 7; see Table 1. Table 2 shows some of the strongest aftershocks along with their arrival time after the 2010 earthquake.

In order to avoid including an aftershock that could correspond to more than one mainshock, we adopted the following selection scheme: If we select an earthquake that occurs at calendar time t_0 as mainshock, then we cannot choose any earthquake that occurs in the interval $(t_0 - T, t_0 + T)$ as mainshock. Furthermore, we consider an earthquake to be a mainshock if the sequence of earthquakes that occur during the following 2 months after its arrival time have strictly smaller magnitudes.

We implemented conditional intensity function estimation using the magnitude of the mainshock as a one-dimensional predictor. Figure 6 shows the estimated conditional intensity

| Magnitude | Number of Earthquakes |
|------------|-----------------------|
| [5.0, 5.5) | 1,679 |
| [5.5, 6.0) | 476 |
| [6, 6.5) | 160 |
| [6.5, 7.0) | 53 |
| [7.0, 9.0) | 25 |

Table 1: Distribution of earthquakes in Chile between 1980 and 2017.

| | | | | | | | |
|-------------------------|-----|-----|-----|-----|-----|-----|-----|
| Magnitude | 6.2 | 6.0 | 6.0 | 7.4 | 6.1 | 6.0 | 6.0 |
| Aftershock Time [hours] | 0.3 | 0.6 | 1.1 | 1.5 | 1.9 | 3.9 | 3.9 |

Table 2: Some of the strongest aftershocks within 4 hours from the magnitude 8.8 earthquake in 27 February, 2010, Chile.

functions (11) for different levels of magnitudes between 5 and 8.5, along with the conditional intensity for the mean magnitude level $x = 6.3$ and for a strong earthquake at magnitude $x = 8.0$. We observe that the conditional intensity function for the strong earthquake has an exponential decay, suggesting that most aftershocks occur closer to the mainshock. The shape of the regression curve thus agrees with the traditional model for aftershock sequences that correspond to large earthquakes, whose intensity function decays as a power law, which is known as the modified Omori law (Daley and Vere-Jones 2003; Utsu et al. 1995).

The regression curve for a magnitude 6.3 earthquake is mostly flat but presents a slow decay towards the end of the time window of observation. This could be due to the fact that medium or low magnitude earthquakes do not tend to produce substantially more aftershocks compared to the natural seismic background activity in Chile. In fact, the conditional intensity function for the strong earthquake is uniformly higher than the one for the magnitude 6.3 mainshock. Finally, the conditional intensity functions for earthquakes below magnitude 6 are mostly flat, which indicates that those earthquakes tend to produce aftershocks that are more uniformly scattered and at least partly correspond to the background seismic activity in Chile.

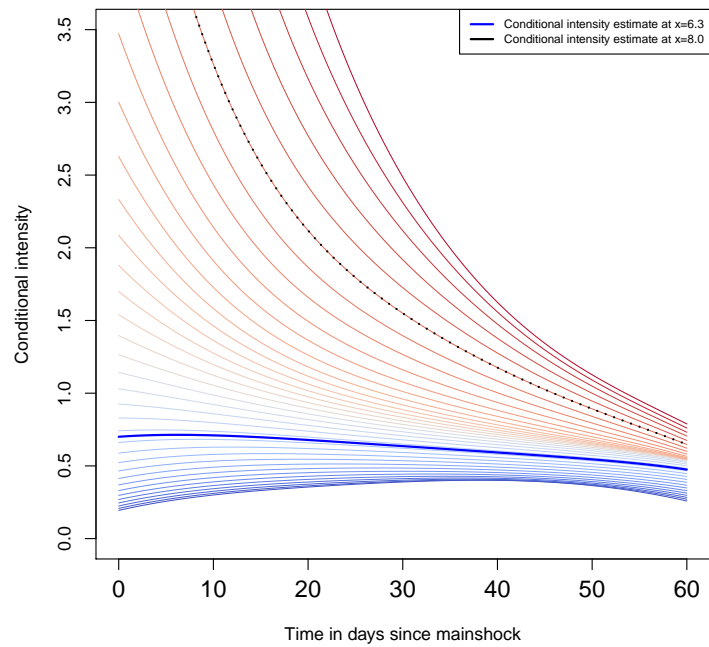


Figure 6: Estimated conditional intensity functions for the aftershock process for different levels of magnitude between 5.0 (blue) and 8.5 (red), with specific conditional intensity functions at magnitudes 6.3 and 8.0, and bandwidth 0.8 in magnitude. The Y-axis is scaled by a factor of 10^{-3} .